Electrochimica Acta 529 (2025) 146328

Contents lists available at ScienceDirect

Electrochimica Acta

journal homepage: www.journals.elsevier.com/electrochimica-acta

On the nature of $K_3Fe(CN)_6$ and $K_4Fe(CN)_6$ in aqueous environment: An ab-initio molecular dynamics study☆

Elisabetta Inico [a,†], Nicole Ceribelli [a,†], Livia Giordano [a], Doriano Brogioli [b], Fabio La Mantia [b,c,**], Giovanni Di Liberto [a,*]

[a] Department of Materials Science, University of Milano-Bicocca, Via Cozzi 55, 20125 Milano, Italy
[b] Energiespeicher-und Energiewandlersysteme, Universität Bremen, Bibliothekstr. 1, Bremen 28359, Germany
[c] Fraunhofer Institute for Manufacturing Technology and Advanced Materials – IFAM, Wiener Str. 12, Bremen 28359, Germany

ARTICLE INFO

Keywords:
DFT
AIMD
Ion pairing
Supporting electrolyte

ABSTRACT

The electron transfer reaction is pivotal in several branches of science, ranging from electrochemistry to catalysis. A suitable model system to inspect to the nature of reactants and products during a charge transfer reaction is made by a redox couple dissolved in a solvent. A typical example is made by $[Fe(CN)_6]^{3-}/[Fe(CN)_6]^{4-}$ in water. Recently, it has been proposed that the charge transfer process is associated with ion-pairing, where counter ions like K^+ take part in the coordination. In this work we performed density functional theory calculations in conjunction with ab-initio molecular dynamics to provide atomistic insights to the structure of $[Fe(CN)_6]^{3-}$ and $[Fe(CN)_6]^{4-}$ in water, and their interaction with K^+. Our results show that $[Fe(CN)_6]^{3-}$ and $[Fe(CN)_6]^{4-}$ display a distinct interaction network with water molecules. The neutrality of $K_3Fe(CN)_6$ and $K_4Fe(CN)_6$ is retrieved by considering a sphere with a radius of about 10 Å, but not more than two K^+ are located closer than 6 Å from the center of the complex. Our estimates indicate that when $[Fe(CN)_6]^{4-}$ is converted to $[Fe(CN)_6]^{3-}$, not only the solvent reorganizes, but also K^+ is reorganized and moves away from the complex by about 0.6 Å. The results may be of help for the fundamental understanding of the nature of this redox couple in water in the presence of supporting electrolyte.

1. Introduction

The electron transfer reaction is pivotal in several fields of fundamental and applied chemistry, ranging from electrochemistry to heterogeneous catalysis [1–4]. During an electron transfer reaction, a reactant is converted to a product via an exchange of electrons in a reaction environment. In real-life applications the reaction environment is extremely complex involving nontrivial sources of electrons [5,6]. The chemical environment around reactants and products can bear both a solvent and a supporting electrolyte, that can be either diluted, modestly or strongly concentrated [7–9]. To understand the chemistry behind the electron transfer reaction, a suitable model system is made by a redox couple immersed in a solvent, in the presence of a supporting electrolyte [10]. This model system has been widely used in the past to deepen the understanding of chemical processes and validate chemical theories [10,11].

In recent years, it has been emerging a relevant effect, named ion-pairing effect [9], in which the nature of the elements of the redox species during the electron transfer process is affected by the amount (concentration) of the co-ions that should be spectators, via the formation of ion-pairs [12]. A key example in this respect is made by the $[Fe(CN)_6]^{3-}/[Fe(CN)_6]^{4-}$. It has been proposed in literature that in water the electron transfer reaction is accompanied by the exchange of a K^+ in the solvation sphere [12,13].

Quantum chemical simulations can be of strong help, allowing to access information at the atomistic level on the structure of species in solution [14–16]. The state-of-the-art methodology is based on density functional theory (DFT). A viable way to account for the dynamic nature of water is to work with DFT in conjunction with ab-initio molecular dynamics (AIMD) simulations [17–19].

☆ The manuscript was written through contributions of all authors.

* Corresponding author.
** Corresponding author at: Universität Bremen, Energiespeicher-und Energiewandlersysteme, Bibliothekstr. 1, Bremen 28359, Germany.
E-mail addresses: lamantia@uni-bremen.de (F. La Mantia), giovanni.diliberto@unimib.it (G. Di Liberto).
† EI and NC equally contributed to this work.

https://doi.org/10.1016/j.electacta.2025.146328
Received 28 February 2025; Received in revised form 11 April 2025; Accepted 25 April 2025
Available online 29 April 2025

In this work, we investigated the nature of $[Fe(CN)_6]^{4-}$and $[Fe(CN)_6]^{3-}$ species and their interactions with water molecules and potassium ions. We focused on the nature of the interaction between the ions and water by invoking static DFT calculations and AIMD. At this aim, initially two static simulations, one for each redox species isolated in vacuum, were performed. After this, in order to explore the interaction with water, a new set of static simulations were performed at an increasing number of water molecules. Moreover, a AIMD simulation were performed, in which one form of the redox pair, i.e. $[Fe(CN)_6]^{4-}$ or $[Fe(CN)_6]^{3-}$, is in presence of water molecules and K^+ ions.

2. Computational details

Density Functional Theory (DFT) calculations have been performed with the VASP [20–22] code using the Perdew–Burke–Ernzerhof parametrization of exchange-correlation functional [23]. Dispersion terms have been introduced using the D3 Grimme's parametrization [24]. The choice of the adopted DFT functional is typically critical when treating chemical systems and water. It has been demonstrated that hybrid functionals containing the exchange and correlation parametrization of the PBE version and suitable dispersion schemes allow them to treat with acceptable accuracy water [15,25,26]. There are several possible solutions for the description of dispersion interactions. Two examples are the Vydrov and Van Voorhis scheme [27–29], or Grimme's dispersion scheme [34]. In the present work, we adopted the latter with the idea to work in the future with electrode/electrolyte interfaces [30, 31]. Previous works showed that comparable results are obtained in the description of the nature of water interfaced with materials by using different dispersion schemes [29,30]. We benchmarked the reliability of our computational approach against B3LYP [32,33] estimates for static calculations of water-complex adducts with increasing number of water molecules involved. Geometry optimizations were performed without imposing any constraints. The valence electrons have been expanded on a set of plane waves with a kinetic energy cutoff of 500eV, whereas the core electrons were treated with the projector augmented wave approach [37,38].

We created simulation cells containing $K_3Fe(CN)_6$ and $K_4Fe(CN)_6$. We modeled a cubic cell having the lattice parameter equal to 1.970 nm, corresponding to a concentration of $[Fe(CN)_6]^{4-}$ and $[Fe(CN)_6]^{4-}$ equal to 0.2 M. This value is higher than the typical one used in experiments, as it compromises between computational costs and reliability of simulation. We simulate neutral cells and compared the results arising from the two different systems, to avoid working with charged cells. We added four and three potassium ions for ferro- and ferri-cyanide respectively, corresponding to $K_4Fe(CN)_6$ and $K_3Fe(CN)_6$ in water solution. The simulation cell contains 249 water molecules. The number of atoms in the working cells are therefore 763 and 764 for $K_3Fe(CN)_6$ and $K_4Fe(CN)_6$ respectively. The Monkhorst−Pack k-point sampling of all calculations was reduced to the gamma point because of cell dimensions [34].

Ab-initio Molecular dynamics trajectories were propagated at a working temperature of 350K and controlled by the Nosé-Hoover thermostat [35,36]. The initial structure of each trajectory was generated by taking the optimized geometry of the ferro- and ferri-cyanide ions and adding a water box with a sufficient number of water molecules to have a concentration of the ions close to 0.2 M. The initial distance between water molecules and the complex was set equal to 3 Å, a value slightly larger than the sum van der Waals radii of N and H (or O) atoms. Trajectories were propagated for 15ps, after equilibration of 1ps. The length of trajectories in AIMD is critical, as long simulation time is needed to correctly sample the configurational space of water [37–39]. Previous works showed that about 8–10 ps trajectories allow to provide some insights on the nature of material/water interfaces [40–44], and to describe the solvation of chemical species [45–47].

3. Results and discussion

3.1. $[Fe(CN)_6]^{4-}$ and $[Fe(CN)_6]^{3-}$ in aqueous environment

The two ions in vacuum display exactly the same structure with nearly the same calculated distances, $d_{Fe\text{-}C} = 1.93$ Å, and $d_{Fe\text{-}N} = 3.11$ Å. Fe is octahedrally coordinated by CN^- in both cases, fully occupying the three degenerate t_{2g} orbitals in $[Fe(CN)_6]^{4-}$. $[Fe(CN)_6]^{3-}$ has one electron less leaving a hole in the t_{2g} orbitals [48]. These values compare with previous data and hybrid calculations reported in Table S1, further justifying the choice of the computational step [48].

We first inspect the interaction between the ions and a single water molecule. The molecule can bind both $[Fe(CN)_6]^{4-}$ and $[Fe(CN)_6]^{3-}$ ions either by coordinating a single CN^- species or bridging two of them, Figs. 1a-1b The latter is more stable by 0.19 eV. The N—H equilibrium distance is 1.69 Å and 2.07 Å for axial and bridge configuration respectively, compatible with the values of hydrogen bonding. increasing the number of water molecules surrounding ferri- and ferrocyanide, we observe that an ordered arrangement is obtained up to six ligands, Figs. 1c-1d The bridge configuration becomes systematically more favorable, as we increase the number of solvent molecules, Figures S1-S2. When we further increase the number of water molecules beyond six, they prefer to arrange in a disordered way around the complex but remaining in the first coordination shell, rather than assuming a more symmetric arrangement in the second coordination shell. Interestingly, in all cases, the Fe-C and Fe-N distances are not sensitive to the presence of water, as it is always equal to $d_{Fe\text{-}C} = 1.93$ Å, and $d_{Fe\text{-}N} = 3.11$ Å respectively. We benchmarked the performance of PBE against B3LYP, finding negligible differences in terms of structure of the adducts and energetics, see Table S1 and Figures S3-S4. This simple test shows that PBE calculations represent an acceptable trade-off between computational costs and reliability of predictions, especially when going towards computationally intensive AIMD calculations, described below.

These calculations indicate that the interaction between water and $[Fe(CN)_6]^{4-}$ and $[Fe(CN)_6]^{3-}$ ions requires including dynamics effects of the solvent, due to the very large number of possible arrangements of water molecules around the complexes, especially when considering a large amount of water molecules (Figure S5).

We performed AIMD simulations of $K_3Fe(CN)_6$ and $K_4Fe(CN)_6$ in water. We start the discussion by looking at the Pair Distribution Function (PDF) between Fe-C and Fe-N atoms for $K_3Fe(CN)_6$ and $K_4Fe(CN)_6$. The plot shows peaks centered at slightly different distances, Fig. 2a. The carbon atoms are about 1.9 Å distant from iron, where $d_{Fe\text{-}C}$ is equal to 1.87 Å and 1.91 Å for $[Fe(CN)_6]^{4-}$ and $[Fe(CN)_6]^{3-}$ respectively, to be compared with the same value calculated without water, 1.93 Å. The nitrogen atoms are about 3.1 Å far from the center of the complex, with $d_{Fe\text{-}N}$ distances equal to 3.05 Å and 3.07 Å for $[Fe(CN)_6]^{4-}$ and $[Fe(CN)_6]^{3-}$ respectively, to be compared with the same value calculated without water, 3.11 Å. Interestingly, the inclusion of dynamic effects of water has an impact on the structure of the ions, and causes an overall shrinkage of both Fe-C and Fe-N distances, depending on the nature of ion, 0.06 Å for $[Fe(CN)_6]^{4-}$ and 0.02 Å for $[Fe(CN)_6]^{3-}$ when looking at Fe-C, and 0.06 Å for $[Fe(CN)_6]^{4-}$ and 0.04 Å for $[Fe(CN)_6]^{3-}$ when considering Fe-N. The same values are nearly unchanged when the complex is surrounded by water molecules within the static approach, Tables S1-S2. The C—N distances are unaffected, Figure S6, and they are always equal to 1.18 Å, both in vacuum and water, for both ferro- and ferricyanide ions.

The difference between the two ions is stronger when looking at the interaction with water. The analysis of the PDF between the nitrogen atoms of the complex and hydrogen atoms of water shows a peak compatible with that of hydrogen bonding [49,50], at $d_{N—H} = 1.83$ Å and $d_{N—H} = 1.87$ Å for $[Fe(CN)_6]^{4-}$ and $[Fe(CN)_6]^{3-}$ respectively, Fig. 2b

A similar trend is found for C—H interactions, with $d_{C—H} = 2.61$ Å and $d_{C—H} = 2.75$ Å for $[Fe(CN)_6]^{4-}$ and $[Fe(CN)_6]^{3-}$ respectively. As a

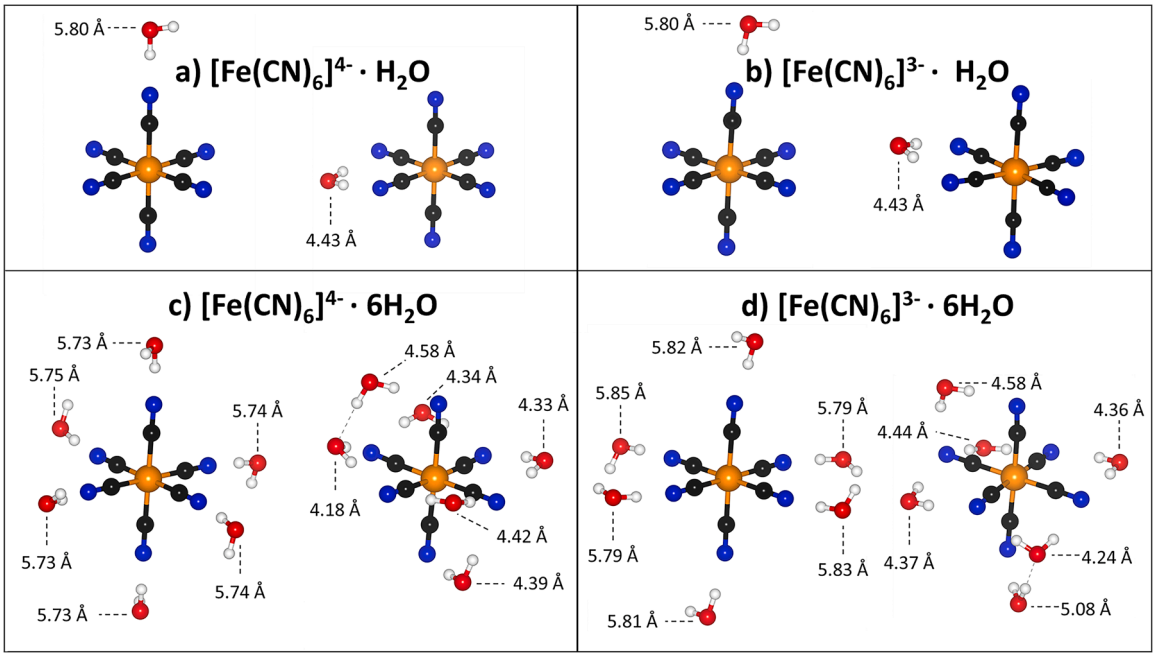

Fig. 1. Interaction of $[Fe(CN)_6]^{4-}$ and $[Fe(CN)_6]^{3-}$ with one (panel a and b) and six (panel c and d) water molecules. For each panel, water interaction with axial (on the left) and bridge (on the right) configuration Is reported. In each panel, the Fe-O distances are reported.

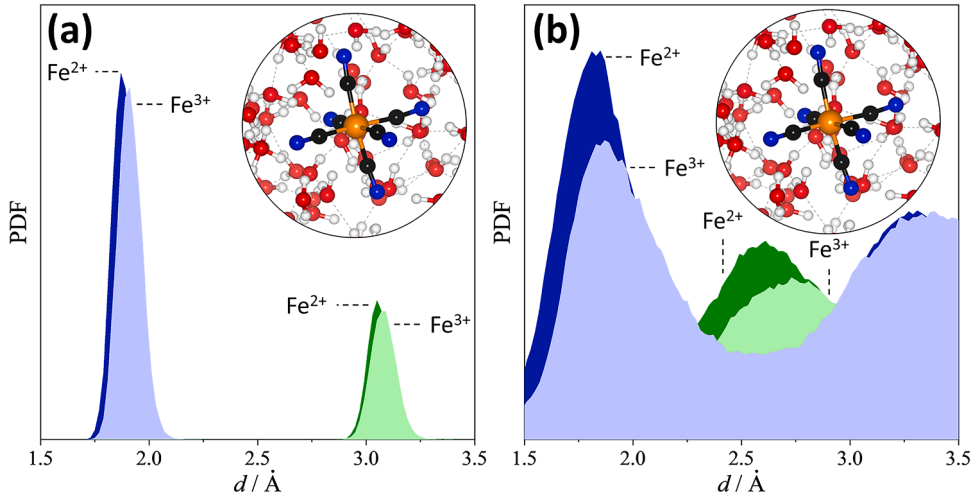

Fig. 2. Panel a is for calculated PDF for the Fe-N (blue) and Fe-C (green) couples in $[Fe(CN)_6]^{4-}$ and $[Fe(CN)_6]^{3-}$. Panel b reports the same but focusing on the interaction with water (N—H in green and C—H in blue).

direct consequence, $[Fe(CN)_6]^{4-}$ is involved in more hydrogen bonding, 1.6 ($[Fe(CN)_6]^{4-}$) and 1.1 ($[Fe(CN)_6]^{3-}$), calculated by integrating the PDF [51]. A similar trend is found by looking at Fe-O interactions, $[Fe(CN)_6]^{4-}$ is surrounded by 16 water molecules and $[Fe(CN)_6]^{3-}$ by 15 water molecules at $d_{Fe\text{-}O} = 5.5$ Å, in line with a previous seminal work by Shao-Horn and co-workers [52]. These results indicate that the two ions display different a local coordination with water molecules, in line with the different charge of the species.

3.2. *Effect of the K^+ counter ion*

Once analyzed the nature of the interaction between the ions and water, we look at the role of K^+. Each simulation cell is neutral to avoid spurious effects due to the simulation of charged cells. Therefore, the cell of $[Fe(CN)_6]^{4-}$ contains four K^+ species, and $[Fe(CN)_6]^{3-}$ contains three K^+ ions. If one starts from initial configurations where all K^+ are close to the complex ($d_{Fe\text{-}K} \sim 6$ Å), interestingly, not all cations are intimately interacting with ferro/ferricyanide, as can be clearly evinced by looking at Figs. 3a-3b, where it is possible to appreciate two different regimes. On one hand, some K^+ directly surround the cyanide with a Fe-K distance oscillating in the range 5–6 Å, which is compatible with the presence of K^+ directly bonding N atoms, Fig. 3d. The number of K^+ simultaneously in contact with cyanide is always oscillating between one and two. Therefore, there is always at least one K^+ (for ferri-) and two K^+ (for ferro-cyanide) distant from the complex, with Fe-K distances larger than 8 Å. The neutrality of the system is retrieved when considering a shell with radius about 9–10 Å, in line with the sum of hydrodynamic radii of K^+ (~3 Å) and $[Fe(CN)_6]^{4-}/[Fe(CN)_6]^{3-}$ (~6–8 Å). The calculated averaged coordination number between the ion and K^+, calculated from the analysis Fe-K PDF (Fig. 3c), is 1.70 ($[Fe(CN)_6]^{4-}$) and 1.25 ($[Fe(CN)_6]^{3-}$) respectively. When K^+ is very far from the cyanide it is surrounded by six water molecules forming the well-known [K

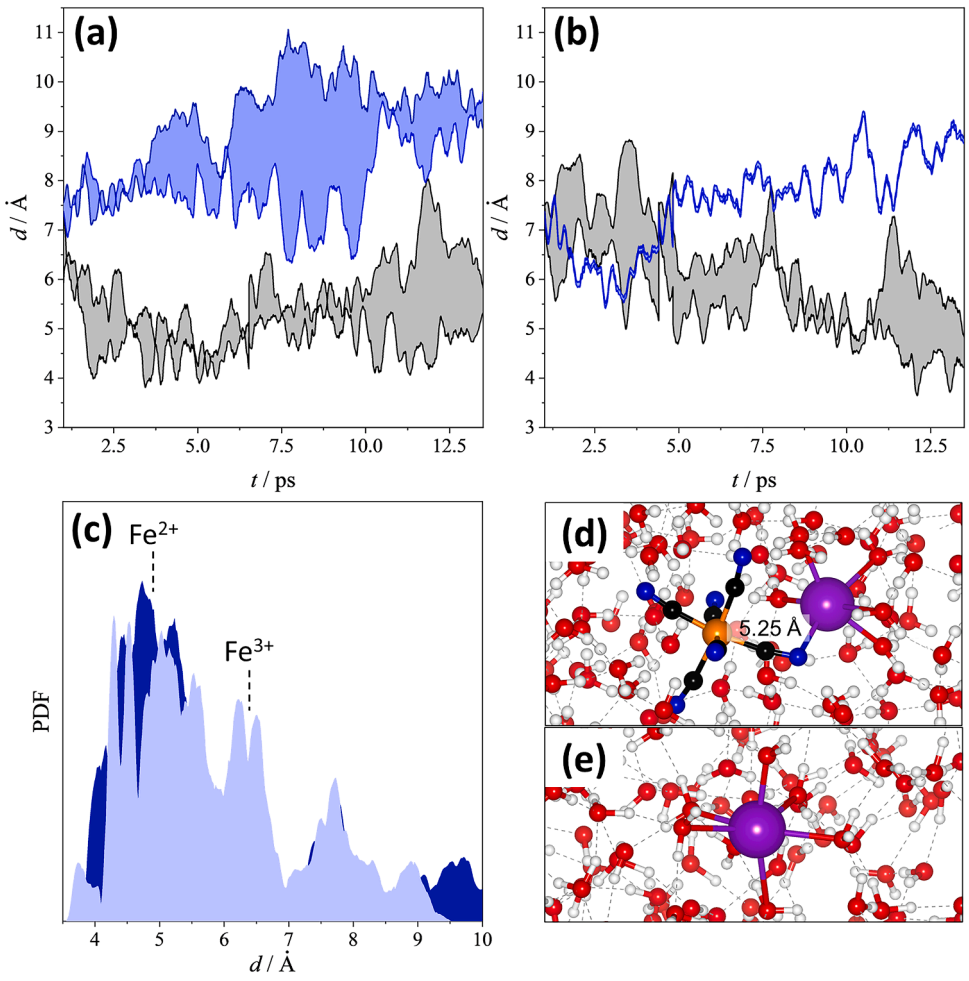

Fig. 3. Instantaneous Fe-K distances along the trajectory of $[Fe(CN)_6]^{4-}$ (panel a) and $[Fe(CN)_6]^{3-}$ (panel b). In panel c the Fe-K PDF is reported, along with snapshots of the possible coordination of the potassium atom: with five water molecules if the complex is present (panel d), with six otherwise (panel e).

$(H_2O)]_6^+$ complex, Fig. 3e.

3.3. Ion pairing

The previous analysis shows that the nature of the interaction between K^+ and the Fe^{2+} and Fe^{3+} complexes is different. Indeed, on average 1.70 ($[Fe(CN)_6]^{4-}$) and 1.25 ($[Fe(CN)_6]^{3-}$) K^+ ions are close to the complex. This value is always two at most during each step of the trajectory with a threshold Fe-K distance of 7 Å, Figs. 3a-3b. The K^+ ions can be found within 10 Å from the complex, but they are not directly interacting with it, and are octahedrally coordinated by water. In other words, there is sort of ion-pairing in an inner sphere within 10 Å from the complex where K^+ is farther from $[Fe(CN)_6]^{3-}$ than $[Fe(CN)_6]^{4-}$. This can lead to the hypothesis that during electron transfer there is both a rearrangement of the solvent around the complex as they have distinct interaction networks in water, and of K^+, that is expected to move away when reducing $[Fe(CN)_6]^{4-}$ to $[Fe(CN)_6]^{3-}$, in line with previous results by some of us [12,53]. Based on the analysis of AIMD discussed below we can estimate that K^+ will move away by about 0.6 Å when $[Fe(CN)_6]^{4-}$ is transformed to $[Fe(CN)_6]^{3-}$.

If one starts from the analysis of the coordination number as a function of the Fe-K distance in $[Fe(CN)_6]^{4-}$ and $[Fe(CN)_6]^{3-}$, one can extract for a specific coordination number, the corresponding Fe-K distances in $[Fe(CN)_6]^{4-}$ and $[Fe(CN)_6]^{3-}$. We label these values as $d_{Fe\text{-}K}([Fe(CN)_6]^{4-})$ and $d_{Fe\text{-}K}([Fe(CN)_6]^{3-})$. Therefore, for each value of the coordination number we can associate the quantity $\Delta d = d_{Fe\text{-}K}([Fe(CN)_6]^{3-}) - d_{Fe\text{-}K}([Fe(CN)_6]^{4-})$. Δd describes on average how different will be the distance between Fe and K species for a given coordination number. Please note that Δd is always a positive number. If we analyze the value of Δd against the coordination number we obtain values in the range 0.6 Å - 0.8 Å when the Fe-K coordination number changes from the value corresponding to that of $[Fe(CN)_6]^{4-}$ (1.70) and $[Fe(CN)_6]^{3-}$ (1.25) respectively, Fig. 4. To corroborate our results, we repeated the analysis but looking at the cumulative average of the Fe-K distance rather than the Fe-K PDF, finding nearly the same results but with a 0.1 Å shift, where Δd assumes values in the range 0.5 Å - 0.7 Å. Therefore, Δd is around 0.65 ± 0.10 Å.

4. Conclusions

We investigated the nature of $K_3Fe(CN)_6$ and $K_4Fe(CN)_6$ in aqueous environment by means of quantum chemical density functional theory calculations, in conjunction with ab-initio molecular dynamics. We started from the analysis of static simulations, showing that the arrangement of water molecules is rather anisotropic, and a large number of water molecules tends to arrange around the complexes. We found that bridging configurations are energetically favourable than axial one. When moving to AIMD, accounting for fluxional behaviour of water results into slightly different internal changes to bond distances of $[Fe(CN)_6]^{4-}$ and $[Fe(CN)_6]^{3-}$. Results show that $[Fe(CN)_6]^{4-}$ and $[Fe(CN)_6]^{3-}$ display a different network of interaction with water. Water molecules are much closer to the $[Fe(CN)_6]^{4-}$ than $[Fe(CN)_6]^{3-}$, as can be seen from the number of hydrogen bonds and the number of water molecules in a coordination shell of radius $r = d_{Fe\text{-}O} = 5.5$ Å. When

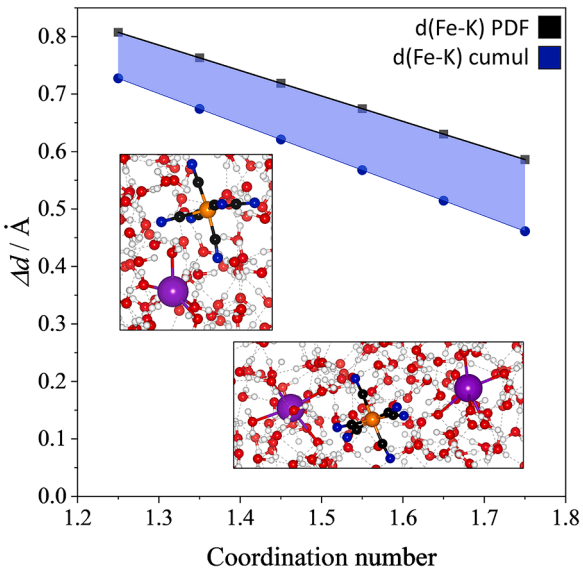

Fig. 4. $\Delta d = d_{Fe\text{-}K}([Fe(CN)_6]^{3-}) - d_{Fe\text{-}K}([Fe(CN)_6^{4-}])$ vs the coordination number. The black points and line are relative to the PDF analysis of the Fe-K distances; the blue points and line of the cumulative average of Fe-K distances.

focusing on the nature of the interaction between K^+ and the ions, it is interesting to observe that not all the cations are in intimate contact with either $[Fe(CN)_6]^{4-}$ or $[Fe(CN)_6]^{3-}$. The maximum number of K^+ directly close to the ion is always smaller than two in any case, with an averaged value equal to 1.70 and 1.25 for $Fe(CN)_6]^{4-}$ and $[Fe(CN)_6]^{3-}$ respectively. The neutrality of the adduct is found when considering a radius of about 10 Å There is ion-pairing in the inner sphere containing the complex water molecules and a few K^+ ions, where the nature of the complex makes the difference. In particular, $[Fe(CN)_6]^{4-}$ has K^+ closer to it than $[Fe(CN)_6]^{3-}$. We finally estimated that the inner sphere will change when $[Fe(CN)_6]^{4-}$ is converted to $[Fe(CN)_6]^{3-}$, where not only is water expected to rearrange, but importantly K^+ will move away by about 0.6 Å from the complex.

Further work will be dedicated to exploring more diluted solutions, by simulating substantially larger simulations cells. This will be possible through the development of suitable force fields or machine learning potentials. This will also allow us to introduce more complexity in the models, such as longer timescales to explore diffusivity and explicit electrode/electrolyte interfaces. Moreover, the study will be extended to other relevant redox couples [54,55].

CRediT authorship contribution statement

Elisabetta Inico: Investigation, Data curation. **Nicole Ceribelli:** Investigation, Data curation. **Livia Giordano:** Writing – review & editing. **Doriano Brogioli:** Writing – review & editing, Validation, Conceptualization. **Fabio La Mantia:** Writing – review & editing, Visualization, Supervision, Conceptualization. **Giovanni Di Liberto:** Writing – original draft, Supervision, Methodology, Conceptualization.

Declaration of competing interest

The authors declare that they have no known competing financial interests or personal relationships that could have appeared to influence the work reported in this paper.

Acknowledgements

Access to the CINECA supercomputing resources was granted via ISCRAB. We also thank the COST Action 18234 supported by COST (European Cooperation in Science and Technology).

Supplementary materials

Supplementary material associated with this article can be found, in the online version, at doi:10.1016/j.electacta.2025.146328.

Data availability

Data will be made available on request.

References

[1] C. Gao, et al., Adv. Mater. 30 (2018).
[2] M.T.M. Koper, Chem. Sci. 4 (2013) 2710.
[3] J. Blumberger, Chem. Rev. 115 (2015) 11191–11238.
[4] H. Sumi, R.A. Marcus, J. Chem. Phys. 84 (1986) 4894–4914.
[5] S. Trasatti, O.A. Petrii, J. Electroanal. Chem. 327 (1992) 353–376.
[6] S. Trasatti, O.A. Petrii, Pure Appl. Chem. 63 (1991) 711–734.
[7] P.N.N. Elumalai, et al., RSC Adv. 14 (2024) 35035–35046.
[8] R. Andreu, F. Sanchez, D. Gonzelez-Arjona, M. Rueda, J. Electroanal. Chem. Interf. Electrochem. 210 (1986) 111–126.
[9] J.J. Watkins, H.S. White, Langmuir 20 (2004) 5474–5483.
[10] N. Elgrishi, et al., J. Chem. Educ. 95 (2018) 197–206.
[11] N.G. Tsierkezos, U. Ritter, Phys. Chem. Liquids. 50 (2012) 661–668.
[12] J. Mugisa, R. Chukwu, D. Brogioli, F.La Mantia, Electrochim. Acta 473 (2024) 143473.
[13] M. Shporer, G. Ron, A. Loewenstein, G. Navon, Inorg. Chem. 4 (1965) 361–364.
[14] A. Pasquarello, et al., Science (1979) 291 (2001) 856–859.
[15] F. Ambrosio, G. Miceli, A. Pasquarello, J. Chem. Phys. 143 (2015).
[16] R.F. de Morais, T. Kerber, F. Calle-Vallejo, P. Sautet, D. Loffreda, Small 12 (2016) 5312–5319.
[17] B. Samanta, et al., Chem. Soc. Rev. 51 (2022) 3794–3818.
[18] P.A. Madden, J. Penman, E. Fois, in: AIP Conference Proceedings, AIP, 1991, pp. 33–47.
[19] A. Roldan, Curr. Opin. Electrochem. 10 (2018) 1–6.
[20] G. Kresse, J. Hafner, Phys. Rev. B 47 (1993) 558–561.
[21] G. Kresse, J. Hafner, Phys. Rev. B 49 (1994) 14251–14269.
[22] G. Kresse, J. Furthmüller, Comput. Mater. Sci. 6 (1996) 15–50.
[23] J.P. Perdew, K. Burke, M. Ernzerhof, Phys. Rev. Lett. 77 (1996) 3865–3868.
[24] S. Grimme, J. Antony, S. Ehrlich, H. Krieg, J. Chem. Phys. 132 (2010) 154104.
[25] F. Ambrosio, G. Miceli, A. Pasquarello, J. Phys. Chem. B 120 (2016) 7456–7470.
[26] W. Chen, F. Ambrosio, G. Miceli, A. Pasquarello, Phys. Rev. Lett. 117 (2016) 186401.
[27] F. Ambrosio, G. Miceli, A. Pasquarello, J. Phys. Chem. B 120 (2016) 7456–7470.
[28] O.A. Vydrov, T. Van Voorhis, J. Chem. Phys. 133 (2010).
[29] R. Sabatini, T. Gorni, S. de Gironcoli, Phys. Rev. B 87 (2013) 041108.
[30] G. Di Liberto, L. Giordano, Electrochem. Sci. Adv. (2023).
[31] R. Jinnouchi, F. Karsai, C. Verdi, G. Kresse, J. Chem. Phys. 154 (2021).
[32] E.R. Johnson, A.D. Becke, Can. J. Chem. 87 (2009) 1369–1373.
[33] A.D. Becke, J. Chem. Phys. 98 (1993) 1372–1377.
[34] H.J. Monkhorst, J.D. Pack, Phys. Rev. B 13 (1976) 5188–5192.
[35] S. Nosé, J. Chem. Phys. 81 (1984) 511–519.
[36] W.G. Hoover, Phys. Rev. A (Coll Park) 31 (1985) 1695–1697.
[37] L.-M. Liu, C. Zhang, G. Thornton, A. Michaelides, Phys. Rev. B 82 (2010) 161415. https://link.aps.org/doi/10.1103/PhysRevB.82.161415.
[38] L.-M. Liu, C. Zhang, G. Thornton, A. Michaelides, Phys. Rev. B 85 (2012) 167402. https://link.aps.org/doi/10.1103/PhysRevB.85.167402.
[39] Z. Ding, A. Selloni, J. Chem. Phys. 154 (2021).
[40] Z. Guo, F. Ambrosio, A. Pasquarello, ACS Catal. 10 (2020) 13186–13195. https://pubs.acs.org/doi/10.1021/acscatal.0c03006.
[41] F. Ambrosio, J. Wiktor, A. Pasquarello, ACS Appl. Mater. Interfaces 10 (2018) 10011–10021. https://pubs.acs.org/doi/10.1021/acsami.7b16545.
[42] P. Gono, F. Ambrosio, A. Pasquarello, J. Phys. Chem. C 123 (2019) 18467–18474. https://pubs.acs.org/doi/10.1021/acs.jpcc.9b05015.
[43] G. Di Liberto, G. Pacchioni, Y. Shao-Horn, L. Giordano, J. Phys. Chem. C 127 (2023) 10127–10133.
[44] F. Maleki, G. Di Liberto, G. Pacchioni, ACS. Appl. Mater. Interfaces 15 (2023) 11216–11224.
[45] N. Daelman, M. Capdevila-Cortada, N. López, Nat. Mater. 18 (2019) 1215–1221. https://www.nature.com/articles/s41563-019-0444-y.
[46] M.C.O. Monteiro, F. Dattila, N. López, M.T.M. Koper, J. Am. Chem. Soc. 144 (2022) 1589–1602.
[47] M.C.O. Monteiro, et al., Nat. Catal. 4 (2021) 654–662. https://www.nature.com/articles/s41929-021-00655-5.
[48] K. Kunnus, et al., J. Phys. Chem. B 120 (2016) 7182–7194.
[49] A.D. Buckingham, J.E. Del Bene, S.A.C. McDowell, Chem. Phys. Lett. 463 (2008) 1–10.
[50] B. Barbiellini, A. Shukla, Phys. Rev. B 66 (2002) 235101.
[51] D. Caprion, H.R. Schober, Phys. Rev. B 62 (2000) 3709–3716. https://link.aps.org/doi/10.1103/PhysRevB.62.3709.
[52] B. Huang, et al., J. Phys. Chem. C 125 (2021) 4397–4411.
[53] E.R. Nightingale, J. Phys. Chem. 63 (1959) 1381–1387.
[54] J.J. Watkins, H.S. White, Langmuir 20 (2004) 5474–5483.
[55] X. Qu, K.A. Persson, J. Chem. Theory. Comput. 12 (2016) 4501–4508.